AM Technology
Unit 18, Berkeley Court,
Manor Park, Cheshire, WA7 1TQ, UK
Tel: +44 (0) 1928 237420
www.amt.uk

Fast Competitive Chemical Reactions within an Agitated Cell Reactor (ACR)

Introduction

In reactor design, the fluid mixing rate can have an important effect on the yield and selectivity of chemical reactions. For slow reactions, the rate of mixing is not a controlling step; therefore, the mixing rate is not important in determining the yield or selectivity. However, for reactions with fast kinetics and especially for fast competitive/consecutive (C/C) reactions, slow mixing rates can limit the overall reaction rate and/or promote slow side reactions relative to fast desired reactions. Thus, for many industrially important fast competitive reactions, slow mixing lowers the yield of desired product(s).

Acid-base neutralization in the presence of organic substrates is the most commonly encountered example where poor mixing can promote undesired side reactions. Neutralization is the desired reaction; however, many organic species are very reactive under high concentrations of acid or base. Rapid mixing will promote the very fast neutralization reaction, whereas slow mixing will allow organic species, in the presence of acids or bases, to react by substitution or decomposition, thereby producing side products. Fast C/C reaction systems are particularly prevalent in the pharmaceutical and specialty chemical industries; Paul [1990] has given several examples of fast C/C chemical reaction systems encountered in the pharmaceutical industry. Fast C/C reactions have been conducted in agitated vessels, agitated vessels with recycle loops and continuous-flow static mixers [Taylor et al., 2005]. In all these cases, the process kinetics and resulting product quality can be determined by the rate and intimacy of contacting the two initially separated fluids.

This study was aimed at determining the competitive nature of the agitated cell reactor (ACR) compared to the devices mentioned above. A pair of competitive reactions has been conducted with two feed locations at various levels of reagent concentrations. The effect of reagent feed time was also investigated.

Literature Review

Competitive /Consecutive (C/C) Reactions
C/C fast reactions are a convenient experimental tool for studying the effect of mixing on chemical reactions. With a C/C system, the reactor effluent composition is suggestive of the mixing effectiveness in promoting desired reactions.

Baldyga and Bourne have had four different classes of competitive and C/C reactions are widely cited for studying the effect of mixing performance on reactor yields. Overviews of the four classes of the Bourne reactions are well documented in Paul et al. [2004]. As shown in Figure 1, mixing of miscible fluids is classified by three length scales: “macromixing” occurs on the scale of vessels, “mesomixing” on the scale of turbulent eddies, and “micromixing” on the scale of molecular diffusion. Kinetic or mechanical energy input into the system aids turbulent mixing and is dissipated by viscous deformation by the following steps: (1) the distribution of fluid by bulk convection (blending); (2) the formation of daughter vortices, which grow and engulf new fluid; and (3) further deformation of daughter vortices resulting to a lamellar structure (momentum diffusion) where molecular diffusion can eliminate regions of segregation in local flow that is laminar (molecular diffusion) [Johnson and Prud’homme; 2003].

AM Technology
Unit 18, Berkeley Court,
Manor Park, Cheshire, WA7 1TQ, UK
Tel: +44 (0) 1928 237420
www.amt.uk

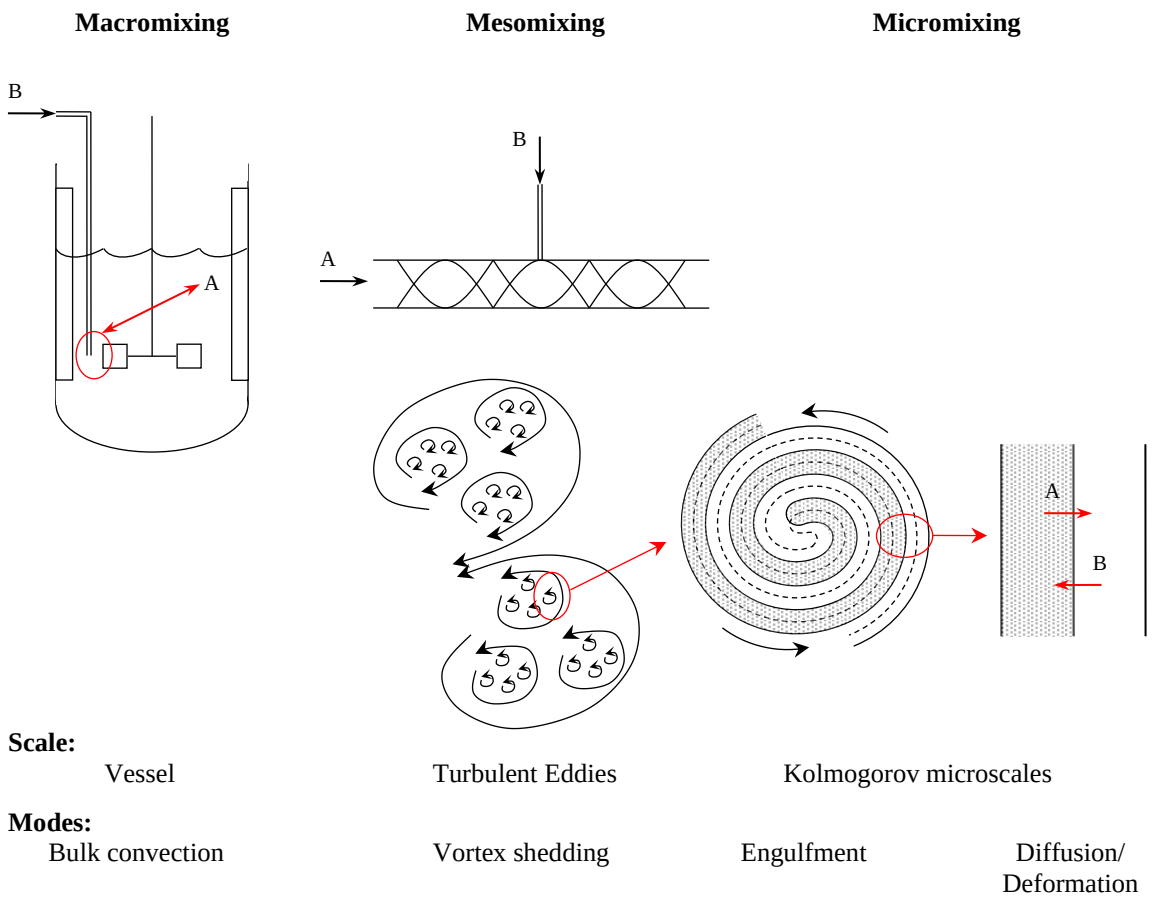

Figure 1. Fluid mixing processes from large to small scales
Portion of graphics for all length scales are from Johnson and Prud'homme [2003].

We can take advantage of the sensitivity and flexibility of chemical reactions in determining the appropriateness the range of equipment types highlighted in this study and expressions for characteristic mixing times obtained within each. Reactions with well defined kinetics are used to characterise the striation length scales and micromixing time [Johnson and Prud'homme; 2003]. The 3rd and 4th Bourne reactions was employed for this study, which is a hydrolysis of either ethyl chloroacetate (ECA) or dimethoxypropane (DMP) reacting in competition with the parallel neutralisation of sodium hydroxide and hydrochloric acid. The 3rd Bourne reaction is approximately 20 times slower than the 4th. These particular schemes were chosen as they are suitable for use in agitated vessels and fast enough for pipeline mixers [Taylor et al., 2005].

$$A + B \xrightarrow{k_1} \text{Products} \quad \text{Fast} \quad \ldots[1a]$$

$$D + B \xrightarrow{k_2} \text{Products} \quad \text{Slow} \quad \ldots[1b]$$

AM Technology
Unit 18, Berkeley Court,
Manor Park, Cheshire, WA7 1TQ, UK
Tel: +44 (0) 1928 237420
www.amt.uk

3rd Bourne reaction:

$$HCl + NaOH \xrightarrow{k_1} NaCl + H_2O$$

$$CH_2ClCOOC_2H_5 + NaOH \xrightarrow{k_2} CH_2ClCOONa + C_2H_5OH$$

4th Bourne reaction:

$$NaOH + HCl \xrightarrow{k_1} NaCl + H_2O$$

$$CH_3C(OCH_3)_2CH_3 + H^+ (+ H_2O) \xrightarrow{k_2} CH_3COCH_3 + 2CH_3OH + H^+$$

Reaction in equation [1a] is inherently instantaneous ($k_1 = 1.4 \cdot 10^8$) and only controlled by micromixing, irrespective of temperature and reagent concentrations. It is irreversible and fairly exothermic (Δh_1 = -55.8 kJ·mol^{-1}). Depending on the local alkaline concentration (for the 3rd Bourne reaction) in equation [1b] is relatively slow and therefore, insensitive to mixing or fast with a mixing-dependant yield. In the case of 4th Bourne reaction, the slower reaction is the acid catalysed hydrolysis of 2,2-dimethoxypeopane (DMP) to form one mole of acetone and two moles of methanol. The following Arrhenius kinetic expression was established for ambient temperature:

$$k_2 = A_0 \cdot \exp^{\left(\frac{-E_a}{R \cdot T}\right)} \qquad \text{...[2]}$$

Where $A_0 = 2 \cdot 10^5$ m^3·mol^{-1}·s^{-1} and E_a = 38.9 kJ·mol^{-1} for the 3rd Bourne reaction and $7.32 \cdot 10^7$ m^3·mol^{-1}·s^{-1} and 46.2 kJ·mol^{-1} for the 4th Bourne reaction. These reactions are also irreversible, and is weakly endothermic (Δh_2 = 18 kJ·mol^{-1}). It is worth noting that both reactions are of second order.

A simple illustration of why these reactions are mixing sensitive is given in Figure 2, by cases: (a) When characteristic mixing time, τ_m, is small relative to the characteristic reaction time, τ_r, of the slow reaction. Here the reaction kinetics approach the homogeneous condition, and since $k_1 \gg k_2$, the fractional yield of the slow reaction, X, is negligible; (b) When the mixing time of reactants is comparable to τ_r, unequal molar ratios exists locally during the reaction. In the interfacial region, reactant A will immediately react with B leaving reactant A depleted locally relative to D. However, reactant D continues to diffuse towards B and has the opportunity to react, therefore X is no longer negligible.

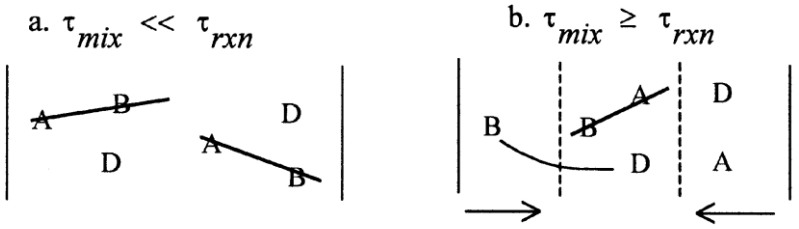

Figure 2. Illustration of micromixing effects on 2nd order consecutive/competitive reactions.
a) Rapid mixing gives negligible conversion of slow reaction; b) detectible conversion led to striations of reactant streams due to mixing.
NB: Reactant B is mixed with a stream of reactants A and D, all at equi-molar.

AM Technology
Unit 18, Berkeley Court,
Manor Park, Cheshire, WA7 1TQ, UK
Tel: +44 (0) 1928 237420
www.amt.uk

The characteristic reaction time, τ_r, can be expressed as the pseudo first-order time constant of the slow reaction [Baldyga and Pohorecki; 1995]:

$$\tau_r = \frac{1}{k_2 \cdot C_{B,0}} \quad \ldots[3]$$

Where the initial concentration of reactant B is the average after mixing as if no reaction had occurred. The product distribution of species D, X_D, which varies from 0 to 1 is defined by the yield of products from the slow reaction relative to the limiting reagent B, that is;

$$X_{EtOH;MeOH} = C_{EtOH;MeOH} \cdot V_{ACR} \Big/ mol_{D,0} \quad \ldots[4]$$

Where $C_{EtOH;\,MeOH}$ is the concentration of the products exiting the reactor for both reactions with $mol_{D,\,0}$ as the initial mols of D entering the system. The yields of the slow reaction products are indicative of the level of mixing. If instantaneous mixing is achieved, none of the D will be reacted. Overall, this is a slow reaction, ideal for in view of studying for a wide range of residence times. Equal residence time is a key scale-up criterion when considering macromixing time scale.

Experimental Apparatus and Operating Conditions

A schematic of the experimental setup is shown in Figure 3. The feeds to the reactor were supplied by a multi-channel peristaltic pump with eight rollers having a flow range of 0.001-230 ml·min^{-1}. Multiple volumetric flow ratios are achievable by attaching tubing's of different internal diameters to the same pump head, i.e. 10:1 and 49.5:1 (main to side) ratios were used in this study. The pump speeds were calibrated prior to each experimental run. The flow rate for the main stream and the injected stream were controlled by specifying a fixed volume to be pumped within a given period of time. The amount of pumped fluids were measured with electronic scales and corroborated. The analysis of the reaction products was performed using a Hewlett-Packard model XXXX series XX gas chromatography (GC) with flame ionization detectors. The GC column was a XX m capillary, which had a XX mm internal diameter. Samples were analysed for ethanol and methanol from the 3rd and 4th Bourne reactions respectively. Samples were collected from the outlet at regular intervals for comparison. However, it was found that the handling of the ECA reaction is less versatile than the DMP reaction, because the minimum characteristic reaction time is limited by the solubility of ECA and the decomposition of ECA can be acid catalyzed prior to mixing the two streams. Thus, reaction solutions were used immediately after adding ethylchloroacetate and reaction effluent samples were immediately diluted with water to slow the reaction and quenched in ice until GC analysis for ethanol. The experimental protocol used for this reaction matches that of the DMP hydrolysis as described above.

AM Technology
Unit 18, Berkeley Court,
Manor Park, Cheshire, WA7 1TQ, UK
Tel: +44 (0) 1928 237420
www.amt.uk

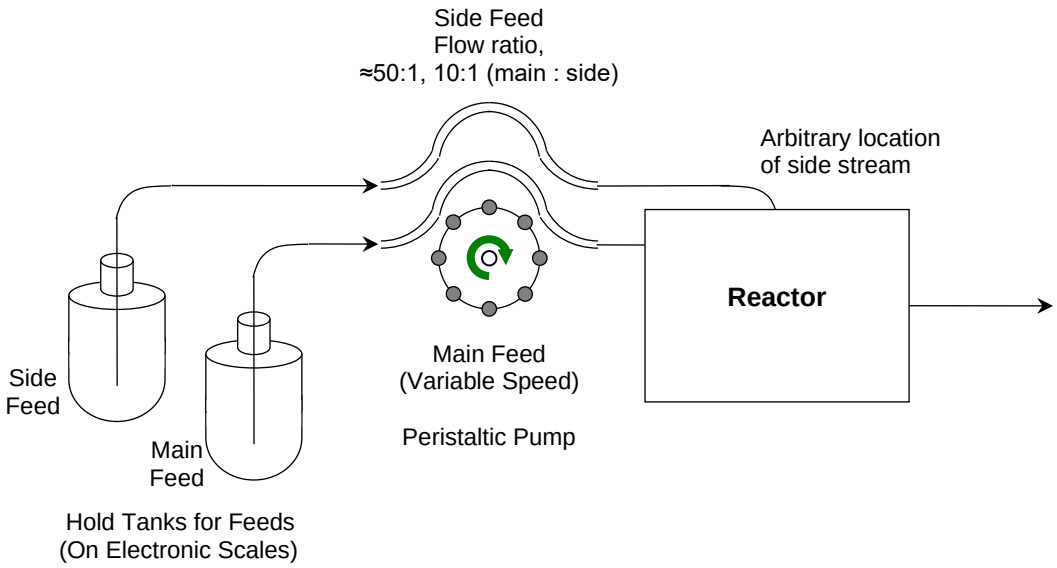

Figure 3. Process flow schematic of the experimental apparatus.

Three reactors were considered in this study, namely: the commonly used batch vessel with stirrer and the Kenics static helical element mixer (HEM), and finally the novel agitated cell reactor (ACR). These are further described below.

ACR

The agitated cell reactor (ACR) consists of ten cylindrical cells in series, each separated by channels with dimensions 30x4x4 mm (Figure 4). The reactor is oriented in a vertical position and so these channels are to act as meso-scale plug flow reactors reducing the effect of back mixing. Each cell has an empty volume of 9.82 ml. Micromixing has a large influence on the product distributions in the reaction zone, a small region where reactants meet and react which deviate from the bulk concentrations [Baldyga et al.; 1998]. The ACR aims to promote micromixing by two means. First, employing agitation elements and second, through oscillation. The reactor is clamped to a mechanically driven arm oscillating the reactor in a lateral direction. This movement intern agitates free moving bodies (elements) within each cell. The volume of each cell can be controlled with displacement from the size of the element. A study is performed on an empty system and one with variable sized elements to suit for the second order nature of the reactions.

The cylindrical reaction cells are bored and the channels are etched into a block of PTFE, respectively. The PTFE block is then housed by a wetted hastelloy heat transfer surface on the rear side. The front side seals the system with borosilicate sight glasses. The injection feed enters either in the 1st cell or the 5th cell (midpoint), normal to the side surfaces (i.e. not edge surfaces) of the cell through stainless steel distributor ports. The main stream enters and exits via channels, similar to those connecting the cells.

Figure 4.agitated cell reactor (ACR)

AM Technology
Unit 18, Berkeley Court,
Manor Park, Cheshire, WA7 1TQ, UK
Tel: +44 (0) 1928 237420
www.amt.uk

The residence time distribution was considered. Unlike static mixers the ACR applies intensive mixing independent to the flow rate. To appropriately characterise the limitations of the system, a typical range of residence times were considered (30 – 500 s; 5.748 – 95.55 ml·min^{-1}). Interestingly, this will also give good understanding of back mixing and flow, especially as the system is orientated vertically with flow travelling upward, thus, working against gravity. A continuous operation of this nature at large residence times may also pose an issue.

Kenics HEM

The Kenics static mixer, introduced in the mid-1960s, is a typical type of static mixer. These static mixers are commercially available in several configurations. This study used a 12-element Kenics HEM of diameter and element length of ¼ inch, thus an element length to diameter ratio of 1, which is depicted in Figure 5. The total length of the mixer is 72 mm, thus allowing for consideration of residence times ranging from 0.03 – 5 s.

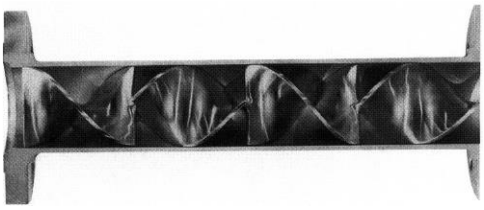

Figure 5. Kenics HEM static mixer

Batch Vessel with Stirrer

Stirred vessels are among the most common reactors used in chemical process industries to carry out a variety of operations, like, homogenisation, gas dispersion, solid suspension, heat transfer, etc [Lin and Lee; 1997]. Over the years many studies have been made to investigate their micromixing characteristics Tipnis et al. [1994], Bourne and Yu [1994], and Nouri et al. [2008] to name a few. Therefore in order to provide a comprehensive study, a standard laboratory batch vessel, i.e. 2 L in capacity, as used in the process development phase within the pharmaceutical sector has been modelled for expected yields and compared to those experimentally found within the novel ACR and the Kenics mixer. A dynamic model has been developed within the gPROMS environment of a stirred tank reactor with a nominal volume of 1.932 L, equipped with a standard Rushton turbine and four baffles placed at 90° intervals (as seen in Figure 1). Both vessel height and diameter were set to 135 mm. The vessel was initially charged with reagents A and D, with reagent B being fed in. The feed in flow rate was manipulated so that the total residence time was 500 s.

The compositions of the main and side feeds with the volumetric flow ratios for all devices are summarised in Table 1.

AM Technology
Unit 18, Berkeley Court,
Manor Park, Cheshire, WA7 1TQ, UK
Tel: +44 (0) 1928 237420
www.amt.uk

Reaction	Feed	Volumetric Flow Ratio (Main:Side)	Material	Inlet Mass fraction	Concentration [mol/m3]
3rd Bourne	Main	-	Hydrochloric acid (HCl)	0.00328	90
			Ethyl Chloroacetate (ECA)	0.01101	90
	Side	10:1	Sodium Hydroxide (NaOH)	0.03533	900
		49.5:1		0.16291	4455
4th Bourne	Main	-	Sodium Hydroxide (NaOH)	0.007997	200
			Dimethoxypropane (DMP)	0.02082	200
	Side	10:1	Hydrochloric acid (HCl)	0.0722	2000
		49.5:1		0.3425	9900

Table 1. Compositions for various main to side volumetric flow ratios

NB: In order to enhance the solubility of DMP in water, the solutes are dissolved in a solvent that is 25 wt.% ethanol.

Discussion of the Results

Here we will discuss operation parameters that influence on the yield of slow products, *X*.

Effect of Residence Time

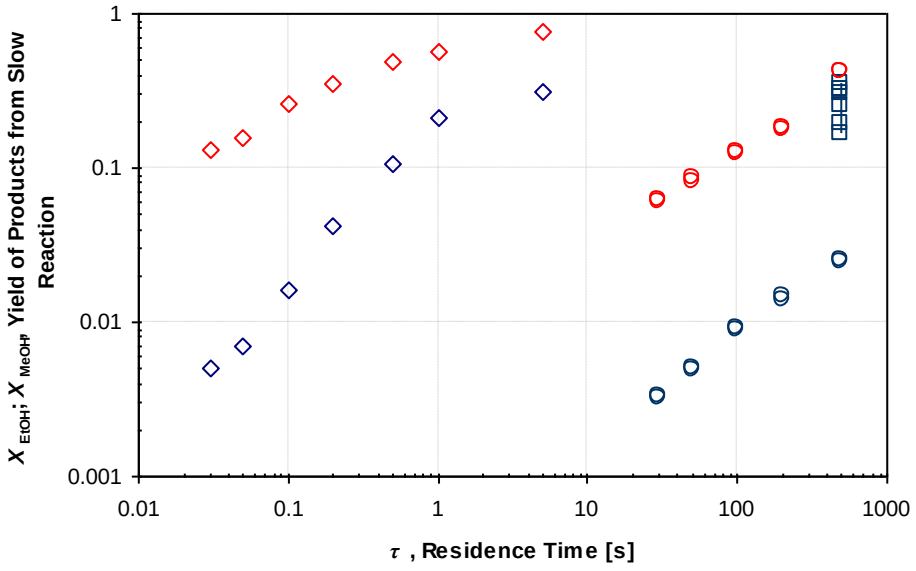

Figure 6. Yield of slow reactions (X_{EtOH}; X_{MeOH}) vs. Residence time (τ)
Legend: ACR (EtOH = ○; MeOH = ○), Kenics HEM static-mixer (EtOH = ◇; MeOH = ◇), batch vessel (EtOH = □).

AM Technology
Unit 18, Berkeley Court,
Manor Park, Cheshire, WA7 1TQ, UK
Tel: +44 (0) 1928 237420
www.amt.uk

All plots within figure 6 indicate that increasing the residence time yields more unwanted product as expected. Larger residence times are yielded within the batch vessel and the ACR compared to the limitation of allowable operation within the Kenics HEM. However, aside from this it is evident that the ACR yields fewer amounts of products (from the slow reactions) in both cases compared to the other devices. The maximum conversion yielded from the ECA reaction is 0.0248, 0.314 and 0.353 within the ACR, Kenics HEM and the batch vessel respectively. This result is consistent with the maximum conversion of ECA of $X = X_{EtOH} = 0.5$, if the fluids were perfectly segregated and a 1:1:1 mole ratio A:B:D was used [Bourne and Yu; 1994]. Interestingly, the behavior of the ACR is very predictable especially comparing to that of the Kenics HEM. The yields of both slow reactions (X_{EtOH}, X_{MeOH}) are governed by the following correlation:

$$X_{\mathrm{EtOH}} = X_{\mathrm{MeOH}} = K \cdot \tau^{\approx 0.7} \qquad \ldots[5]$$

Where constant, K, is ≈0.0003 and ≈0.006 for the 3rd and 4th Bourne reaction respectively. This also confirms that the 4th Bourne reaction is approximately 20 times faster than the 3rd.

The batch vessel was only applied to the 3rd Bourne reaction, as it is around 20 times slower than that of the 4th, and shows constant residence time as the reacting stream was fed at a constant rate (≈5.667 ml·min^{-1} for τ = 500 s), although blend time varies due to the impeller speed.

It is worth noting that the highest Reynolds in the Kenics HEM is ≈12800, whereas in the ACR it is envisaged to be lower; thus, it is expected that at the same residence time, the Kenics HEM would out perform the ACR because the flow is considerably more turbulent. However when considering scale-up, an equal residence time keeps the actual time scales constant and seems to be the most prudent criterion as it is expected to be conservative.

Effect of the Reynolds Number

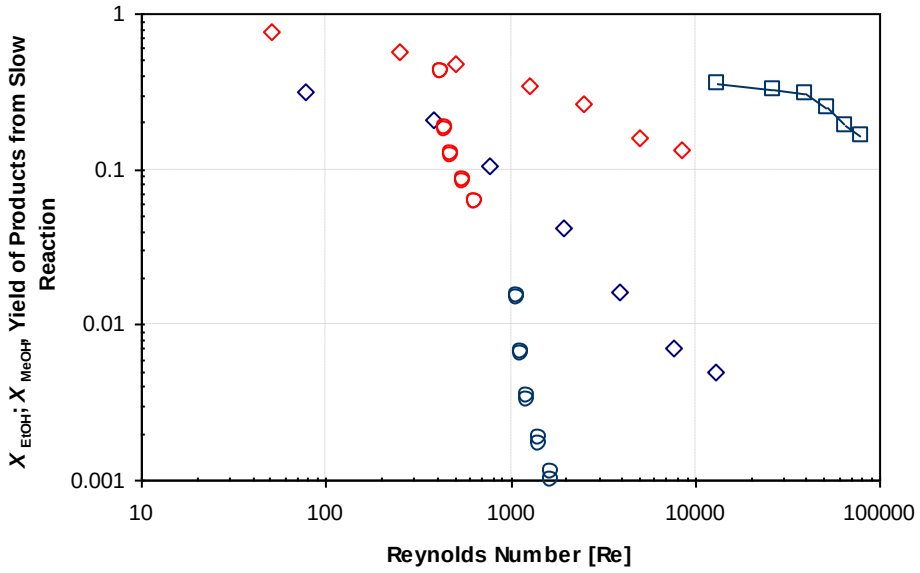

Figure 7. Yield of slow reaction (X_R) vs. Reynolds number (Re) for all reactors at various residence times, τ.

AM Technology
Unit 18, Berkeley Court,
Manor Park, Cheshire, WA7 1TQ, UK
Tel: +44 (0) 1928 237420
www.amt.uk

Legend: ACR (EtOH = ○; MeOH = ○), Kenics HEM static-mixer (EtOH = ◇; MeOH = ◇), batch vessel (EtOH = □).

Yields analysed by gas chromatography for the range of residence are presented graphically against the Reynolds numbers of all three reactors, *X* vs. Re (Figure 7).

Transitional mixing mechanism of mixed layers and eddies are evident under the tested operating conditions within the ACR, created from kinetic energy dissipation from flow rate and the oscillating motion. Similar Reynolds numbers for both the batch vessel and for the Kenics HEM (4th Bourne reaction) have been reported [Tipnes et al.; 1994, Taylor et al.; 2005].

As expected all plots show yield of slow products decreases with increasing Reynolds number. This is likely a result of the data bridging the transition regime of the increasing Reynolds, due to an increase in the mixing rate from the flow becoming more turbulent, therefore, more kinetic energy being dissipated.

The batch vessel shows Reynolds at different impeller speeds which uphold similar gradients to the Kenics HEM. Unlike the Kenics HEM however, the Reynolds within the ACR increases independent of the stream velocity from the intensity of lateral oscillations, as seen by steep gradient. This point is further emphasized by shape of the curves Figure 8, where Reynolds numbers are determined for an ACR with and without oscillations for the range of residence times. At equal Reynolds, there is a large advantage for the ACR as the residence time is much larger, more like a semi-batch approach as opposed to a purely continuous, advantageous when considering process controllability.

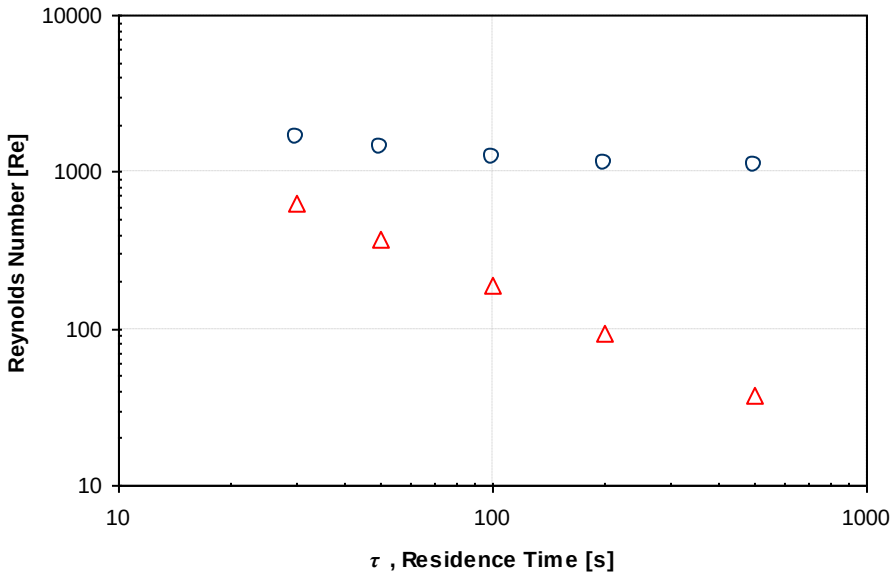

Figure 8. Reynolds number (Re) vs. Residence time (τ), at two oscillating frequencies, highlighting Re independent of flow rate.
Legend: 130 osc.·min^{-1} = 2.167 Hz (○), 0 osc.·min^{-1} = 0 Hz (△)

The batch vessel for various impeller speeds (*N*) remains entirely in the turbulence regime. The Kenics HEM bridges the transition regime for pipe flow. Reynolds numbers determined for the ACR are within the transition regime, and below full turbulence of 10^4 assuming the cells behave similar to impeller driven batch vessels [Tatterson, 1994]. To typify the contribution of Reynolds against the other reactors in Figure 7, average values for the system as a whole were given at the observed residence times. However, a truer representation

AM Technology
Unit 18, Berkeley Court,
Manor Park, Cheshire, WA7 1TQ, UK
Tel: +44 (0) 1928 237420
www.amt.uk

indicates the broad range of Reynolds (within the ACR) for a range of residence times whilst oscillating at the maximum frequency of 130 osc.·min^{-1} (Figure 9).

The ACR is able to configure the internal geometry to the reaction scheme, thus matching closely to the process. The Reynolds number within each cell would also vary. For example, in the same way the active volume within the successive cells increases, the corresponding Reynolds also increases, as seen by the plots for Reynolds at typical residence times of 30 and 500 s for both 3rd and 4th Bourne reactions (Figure 9).

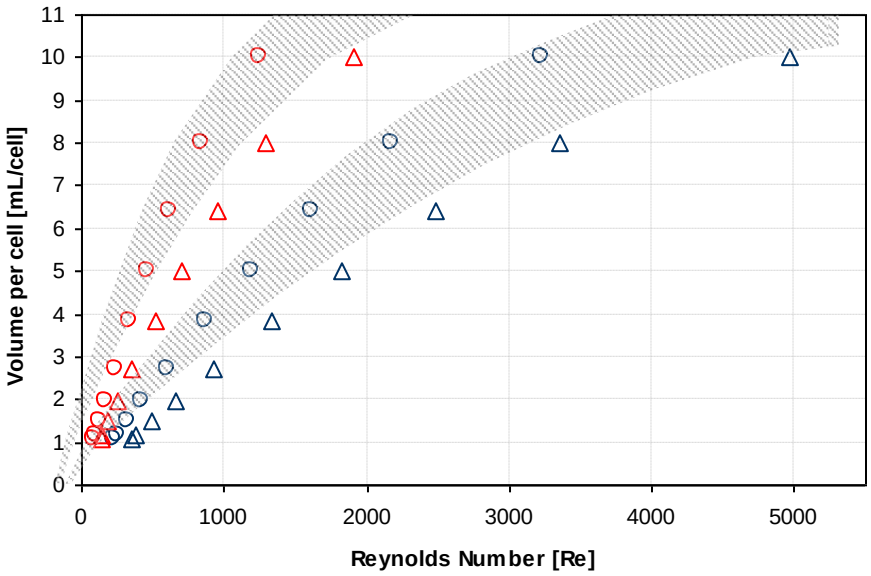

Figure 9. Active volume per cell (V_{cell}) vs. Reynolds number (Re), highlighting polynomial plots at given Re.
Legend: 3rd Bourne reaction (500 s = ○; 30 s = △), 4th Bourne reaction (500 s = ○; 30 s = △).

The calculation of Reynolds within the cells of the ACR was based on a well-known empirical relation:

$$\mathrm{Re}_{\mathrm{ACR}} = \frac{\vec{\upsilon} \cdot D_{\mathrm{agitator}} \cdot \overline{\rho}}{\overline{\mu}} \qquad \ldots[6]$$

Where, v and $D_{agitator}$ are the velocity component (m·s^{-1}) and diameter (m) of agitator element respectively. Consider a typical cell; the velocity term is a combination of the velocity entering the cell from the preceding plug flow channel, and the velocity of the free-moving agitator element created by the oscillating ACR (Figure 10). To simplify the mechanism, the agitator element is assumed to behave similar to that of an impeller, and so has an angular velocity which agitates the surrounding fluid. Both components compliment each other as they travel in the same direction:

$$\vec{\upsilon} = \vec{\upsilon}_{\mathrm{in}} + \vec{\upsilon}_{\mathrm{agitator}} = \left(\frac{\dot{m} \cdot A_{\mathrm{channel}}}{\overline{\rho}} \right) + \left(\omega_{\mathrm{agitator}} \cdot R_{\mathrm{cell}} \right) \qquad \ldots[7]$$

AM Technology
Unit 18, Berkeley Court,
Manor Park, Cheshire, WA7 1TQ, UK
Tel: +44 (0) 1928 237420
www.amt.uk

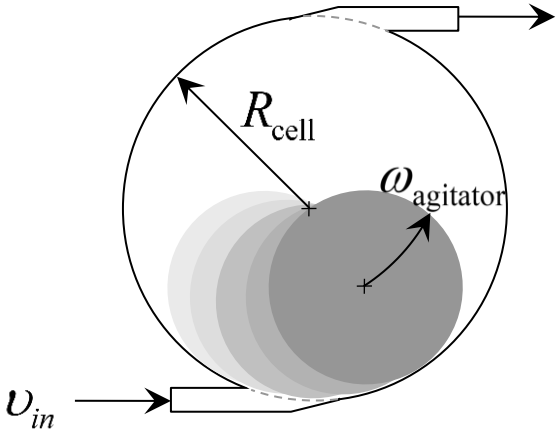

Figure 10. Cell with free moving agitator element and inlet and outlet plug flow channels. Arrows indicate the direction of the velocity components.

Micromixedness Ratio (α)

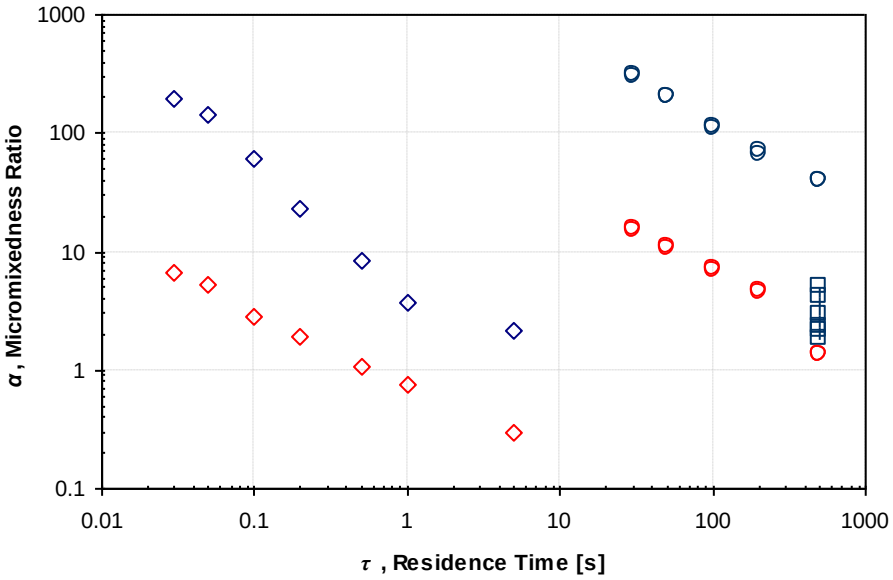

Figure 11. Micromixedness ratio (α) vs. Residence time (τ)
Legend: ACR (EtOH = ○; MeOH = ○), Kenics HEM static-mixer (EtOH = ◇; MeOH = ◇), batch vessel (EtOH = □).

AM Technology
Unit 18, Berkeley Court,
Manor Park, Cheshire, WA7 1TQ, UK
Tel: +44 (0) 1928 237420
www.amt.uk

The micromixedness ratio (α) is defined as the ratio of perfectly mixed volume to a totally segregated volume in the system, and is calculated by the following expression:

$$\alpha = \frac{V_{\text{Perfectlymixed}}}{V_{\text{Totallysegregated}}} = \frac{1-X}{X} \qquad \text{...[8]}$$

High values of α indicate good micromixing, low values therefore imply poor micromixing. This ratio is interesting as it is closely related to the ratio of two characteristic times: τ_r, reaction time and τ_m, micromixing time [Fournier et al; 1996].

In all systems α decreases with increasing τ, thus the influence of improving mixing on product distribution is both demonstrated and quantified (Figure 11). As one would expect, the micromixing intensity constantly decreases with increasing residence times as seen for all cases (when α starts reducing, entering into macromixing conditions). In stirred batch reactors of similar volumes, Tipnes et al. [1994] have yielded similar α values for the 3rd Bourne reaction to those of this study, as do the α values of the Kenics HEM of the 4th Bourne reaction to results from Taylor et al. [2005]. The comparison of effectiveness ratio (α) with the other devices shows that the ACR is characterised by a high micromixing efficiency. The cell reactor out performs the stirred batch vessel in all conditions, whereas to some extent comparable to the Kenics mixer. For example, consider the 4th Bourne reaction at a residence time of 100 s, a value of ≈7 is achieved for the α within the ACR. Similar values are obtained within the Kenics mixer at the largest observed inlet velocity giving a residence time of 0.03 s.

To be able to truly quantify the influences on micromixing, the energy dissipation rate, ε, into the bulk fluid must be the controllable parameter and evaluated to the micromixedness ratio, α. The energy dissipation rate seems not only to be a good criterion for scale-up of micromixing efficiency in reactors, but also, a criterion for the comparison of micromixing efficiency, independent of feed location, in different of geometries of reactors [Nouri at al.; 2008]. This rate is straightforward to determine within the Kenics mixer and the batch vessel through accepted power laws that take the form:

$$\alpha \propto a \cdot \varepsilon^{b} \qquad \text{...[9]}$$

Such power laws proportionally relate the energy dissipation rate to the micromixedness ratio, which characterises the kinetic energy dissipated within the system through determining constants a and b. For example, by varying the inlet stream velocity within the Kenics mixer and the impeller speed of the batch vessel.

However, within the ACR, energy dissipated to the bulk fluid is from three means, from;

- the inlet stream velocity into the system
- the internal geometrical orientation. Consider a particle within the bulk fluid entering the system from the inlet. The particle passes through a constricting region of the connecting channel which has unidirectional, laminar flow. Then expanding into the space within the cell which renders the particle the freedom to a turbulence regime from a velocity field with non-zero curl. Thereafter, the particle is once again subjected to the constricting channel, and so on.
- the frequency of oscillating movement of the ACR structure. This primarily agitates the bulk fluid (hence the particle) through lateral pendulum like oscillations of the free moving elements within the cells.

From these findings it is conceivable that an accurate measure of the dissipation rate is relatively complex at best. Nevertheless, the oscillatory movement dissipates a greater amount of energy to that of increasing the stream velocity as the perpendicular velocity (to the upward flow) of the ACR structure is ten times faster at its

AM Technology
Unit 18, Berkeley Court,
Manor Park, Cheshire, WA7 1TQ, UK
Tel: +44 (0) 1928 237420
www.amt.uk

highest observed frequency (2.167 Hz $\Rightarrow$ 130 osc.·min^{-1} $\Rightarrow$ 0.065 m·s^{-1}) than its equivalent stream velocity for a τ = 500 s (Figure 12). An analysis of the micromixedness ratio, α, determined from ethanol yields of the 3rd Bourne reaction to varying oscillation frequencies was carried out. Noticeably by increasing the frequency has a positive impact of the effectiveness of micromixing in all residence times, and by a factor of ten at τ = 30 s. Importantly, this boasts that the energy dissipation rate can be increased and be independent of the stream velocity, allowing for large residence times with an extremely good of mixing. This is highly desirable within the pharmaceutical sector where flexibility of operating conditions adds value.

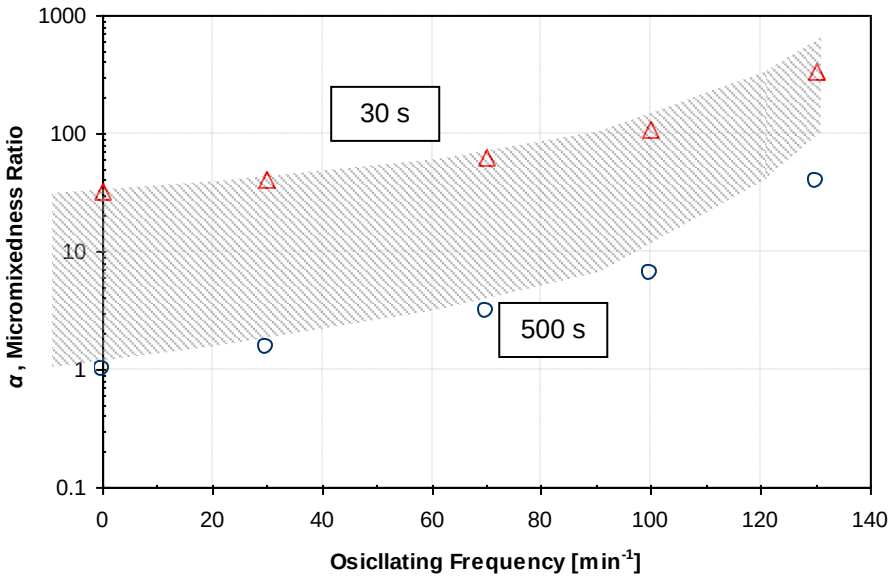

Figure 12. Micromixedness ratio (α) vs. Oscillating frequency (min^{-1}), highlighting exponential plots at the minimum and maximum residence times.
Legend: 500 s (○), 30 s (△).

AM Technology
Unit 18, Berkeley Court,
Manor Park, Cheshire, WA7 1TQ, UK
Tel: +44 (0) 1928 237420
www.amt.uk

Effect of injection position of secondary stream at Cell 5 (midpoint)

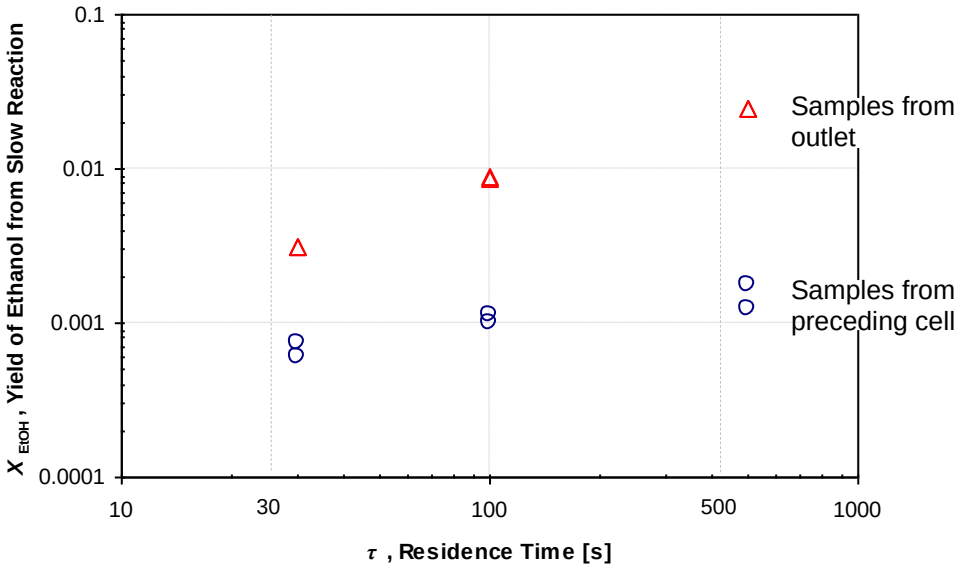

a.

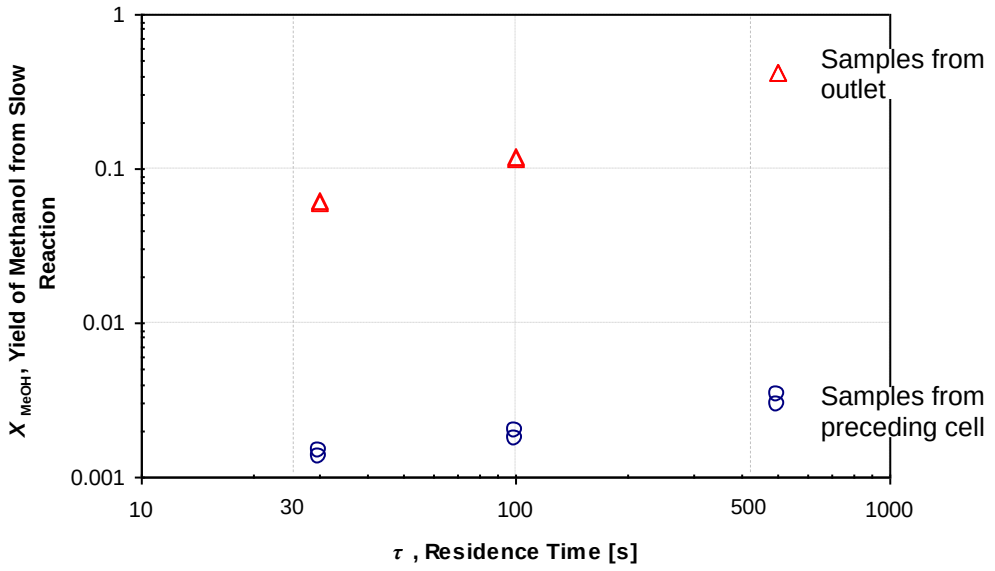

b.

Figure 13. Yield of slow reaction (X_R) vs. Residence time (τ), for the 3rd Bourne reaction (**a.**) and the 4th Bourne reaction (**b.**).
Legend: Samples taken from Cell 4 (○), Samples taken from reactor outlet (△)

The ACR is vertically orientated so that gravity aids in its operation through upward flow. Upward flow achieves a fully immersed system with low pressure drop, when dealing with fully liquid phase medium. However, it is clear that backflow is a concern. In theory, the plug flow channels that connect the cells are orientated to enable forward flow. The presence of minimal backflow was validated by introducing the

AM Technology
Unit 18, Berkeley Court,
Manor Park, Cheshire, WA7 1TQ, UK
Tel: +44 (0) 1928 237420
www.amt.uk

reacting side stream at an arbitrary location, e.g. at the midpoint, cell no. 5. The main and side streams were held at the corresponding volume flow ratios (main to side = 49.5:1) for all residence times. A sample was thereafter collected from the reactor effluent and from the preceding cell (cell no. 4). As before, both reactions were performed and the samples analysed by gas chromatography for ethanol and methanol content.

Figure 13 undoubtedly indicates good forward momentum within the ACR, with methanol content being two orders of magnitude less than the reactor outlet sample for the 4th Bourne reaction. However, due to the potency of sodium hydroxide the samples taken from the 3rd Bourne reaction show one order of difference in magnitude between both samples. As the residence time increases the samples from cell no. 4 also highlight an increase in the yield of slow products as expected, but surprisingly the increase is incremental. An explanation can be hypothesised from the prevailing direction of flow, i.e. perpendicular to the vertical, from the lateral frequency of oscillations (2.167 Hz for this study). The orientation of the connecting plug flow channels also play a vital role. It is worth noting that the fast kinetics of both reactions displays similar yields from reactor effluent samples to those found earlier.

Effect of various oscillation frequencies

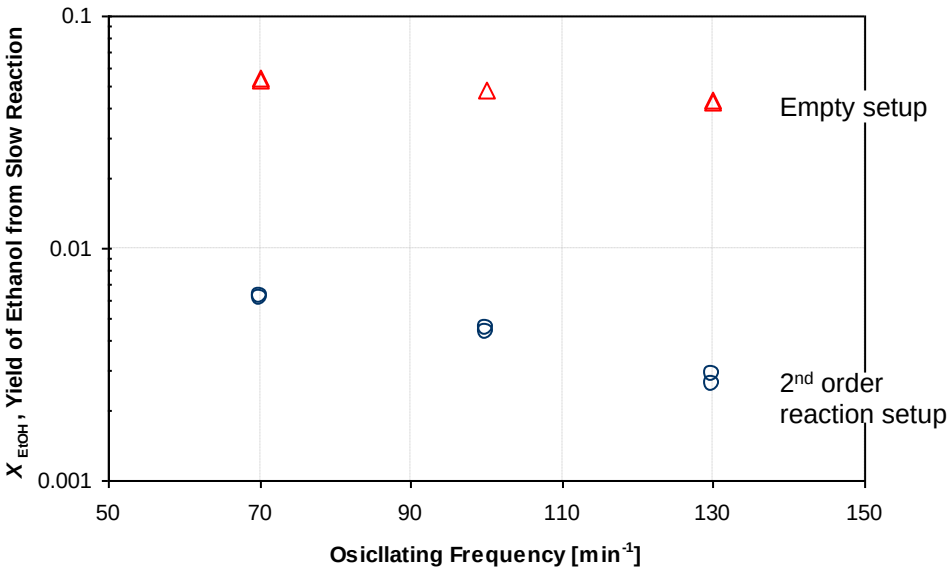

Figure 14. Yield of slow reaction (X_{EtOH}) vs. Oscillating Frequency
Legend: Reactor setup to 2nd order configuration (○), Empty reactor (△)

An experimental analysis was conducted to quantify the relevance of the agitator elements. As before, the 3rd Bourne reaction was performed in an empty setup and with agitator elements within each of the reaction cells, both to increasing oscillations. Both rate constants within the 3rd Bourne reaction are 2nd order, and thus the agitator elements were accordingly sized through pre-experimental models to give equal conversion within each of the ten cells within this setup, i.e. 10 % after the 1st cell, 20 % after the 2nd cell, and so on. A residence time of 200 s was set with a volume flow ratio of 10:1 (main to side). Samples collected at the reactor outlet were subsequently analysed.

The findings highlight that without the agitator elements there is propensity away from micromixing and towards macromixing (Figure 14). Increasing the oscillation frequency from 70 to 130 osc.min^{-1} within the

empty setup has a negligible effect on the yield of ethanol, as can be seen by the near horizontal gradient. This can be accounted for by the bulk fluid moving side to side with the oscillations of the ACR structure, thus acting as a single rigid body, with the inertia of the fluid having little or no impact on the mixing. On the other hand, the agitator elements implicate micromixing conditions, which is clearly evident with the large decrease in yields with the increase of oscillation frequency. The agitator elements are free moving bodies, and as expected, the side to side movement "agitates" the elements which agitate the fluid within the reaction cells.

Pressure Drop (ACR vs. Static mixer)

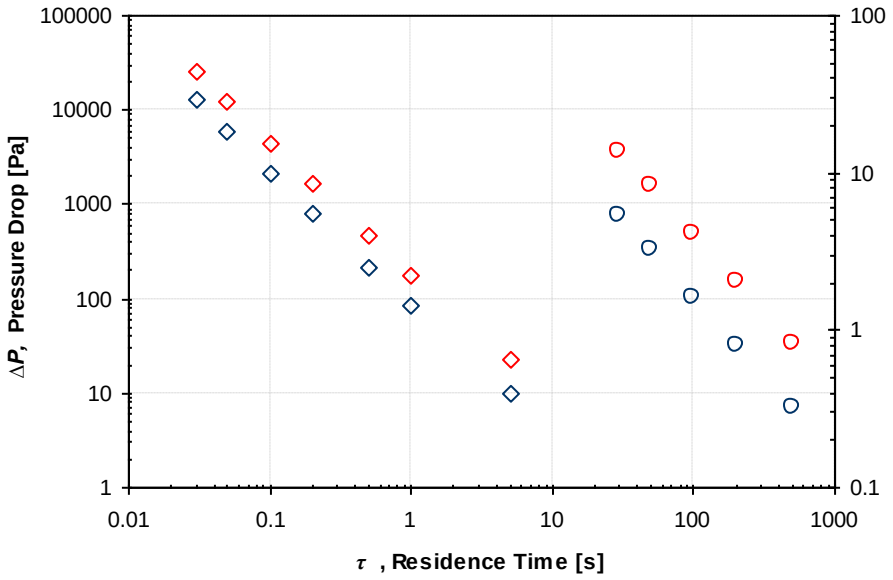

Figure 15. Pressure drop (ΔP) vs. Residence time (τ)
Legend: ACR (EtOH = ○; MeOH = ○), Kenics HEM static-mixer (EtOH = ◇; MeOH = ◇)

Despite the various advantages of the Kenics static mixers, its use can often be restricted due to the substantially large pressure drop caused by the helical elements. It might be envisaged that the mixing strength of the Kenics static mixer is achieved at the expense of high pressure drop. In this regard, it is an important issue to make a reliable pressure drop correlation in the Kenics mixer to the ACR. The benefits of *a priori* estimating pressure drop are straightforward. In a designing stage, it is a prerequisite to calculate the power of the pump. Besides, pressure drop estimation is valuable in determining the possible operating window of the mixer/reactor.

The pressure drop within the Kenics mixer was calculated on the basis of three dimensionless groups, i.e. friction factor, Reynolds, and element length to diameter ratio [Song and Han; 2005] and confirmed from a geometry with and without packing [Boss and Czastkiewicz; 1982]. The pressure drops of both reactors are measured against the monitored residence times, Kenics mixer on the left y-axis and ACR on the right y-axis (Figure 15). The early assumptions of mixing strength within the Kenics mixer are quantified from the ΔP especially at the lower residence times. On the contrary the ACR, due to its upward flow, utilises a much lower pressure drop, whilst maintaining a high level of mixing intensity.

AM Technology
Unit 18, Berkeley Court,
Manor Park, Cheshire, WA7 1TQ, UK
Tel: +44 (0) 1928 237420
www.amt.uk

Through systematic graphical analysis, we successfully obtain curves describing the pressure drop characteristics in the Kenics static mixer and the ACR, from the following power relation:

$$\Delta P_{Kenics} = \Delta P_{ACR} = c \cdot \tau^{d} \quad \text{...[10]}$$

Where constant *d* is ≈-1.4 and ≈-1 for the Kenics mixer and the ACR respectively. However, constant *c* is determined on the basis of the above mentioned dimensionless groups for the Kenics mixer, whereas the ACR utilises the superficial stream velocity instead of the element length to diameter ratio. The proposed pressure drop correlation is distinguished from the existing correlations by the fact that it applies to the whole range of Reynolds from laminar to turbulence.

Analysis Considering Micro- and Mesomixing Time Scales

The 1941 theory of Kolmogorov introduces the idea that the smallest scales of turbulence are universal (similar for every turbulent flow) and that they depend only on energy dissipation rate, ε, and kinematic viscosity, ν [Pope; 2000]. The definitions of the Kolmogorov microscales can be obtained using this idea and dimensional analysis. Since the dimension of kinematic viscosity is length^2/time, and the dimension of the energy dissipation rate per unit mass is length^2/time^3, the only combination that has the dimension of time is $\tau_\eta = \left(\nu/\varepsilon\right)^{1/2}$ which is the Kolmogorov time scale. The time scales (or time constants) identified by Baldyga, Bourne and Hearn [1997] are adapted from Kolmogorov and presented here as Equations 11-13, used here for determining the appropriate time scales.

In liquids, the "engulfment" of new fluid is the rate limiting step in micromixing [Equation 11] and not molecular diffusion has been shown by Baldyga and Bourne [1989];

$$\tau_e \cong E^{-1} \cong 17.31 \cdot \left(\frac{\nu}{\varepsilon}\right)^{1/2} \quad \text{...[11]}$$

Two mesomixing mechanisms have been identified: a) turbulent dispersion, whereby a feed stream spreads out transverse to its local streamline with a time constant of τ_d;

$$\tau_d \cong \frac{Q_2}{\upsilon \cdot \xi \cdot N_F} \quad \text{...[12]}$$

And b) the inertial convective turbulent dispersion of the entering feed, τ_S:

$$\tau_S \cong 2 \cdot \left(\frac{\Lambda_C^2}{\varepsilon}\right)^{1/3} \quad \text{...[13]}$$

Where, Q_2 is the volumetric flow rate of the side stream, υ is the superficial liquid velocity, ξ is the turbulent diffusivity, and N_F is the number of side feed ports. The integral scale of concentration fluctuations, Λ_C, can be

AM Technology
Unit 18, Berkeley Court,
Manor Park, Cheshire, WA7 1TQ, UK
Tel: +44 (0) 1928 237420
www.amt.uk

described by the cascade in the concentration spectrum. When a spot of pure, unmixed solution is mixed by a turbulent flow, the velocity fluctuations of smaller scale distort this sport and produces concentration fluctuations (see Figure 1 in Baldyga et al. [1997]).

Comparison of time constants allows a controlling mechanism to be identified, i.e. comparing micro- and mesomixing, the influence of viscosity on micromixing is evident in Equation 11. It is also worth noting that as ε increases, τ_e decreases faster than τ_s, which suggests a change in controlling mechanism from micro- to mesomixing. An example of this shift would be by increasing the feed rate or impeller speed if considering a semi-batch operation. Subsequently, we will illustrate the controlling mechanism within the ACR.

Figure 16 displays the characteristic times that have the same scaling as momentum diffusion.

$$\propto \left(\nu / \varepsilon\right)^{1/constant}$$

Figure 16. Characteristic time, (s) vs. Reynolds number (Re), thus the residence time in the ACR, Legend:

Conclusions

The 3rd and 4th Bourne reactions were used as a means of comparing the performance of standard mixing equipment, i.e. batch vessel with stirrer and Kenics static mixer, to the novel agitated cell reactor (ACR). The chosen test reactions are sufficiently fast, with the 4th Bourne being approximately 20 times faster than the 3rd, to allow investigation within the three equipages already mentioned. The effect of residence times, Reynolds numbers, micromixedness ratio, pressure drop, side stream feed locations were characterised. All results seem to be reliable with high reproducibility, due to simple experimental procedure.

The results obtained within the ACR indicate a higher level of mixing efficiency than the other devices for both reactions, especially for the slower 3rd Bourne. The high level of power dissipation is an acceptable criterion for micromixing control, while control of the residence time is a conservative approach to mesomixing conditions. High level of mixing, indicative of the micromixing scale is achieved whist having a large operating window in terms of the residence time. The power dissipated from varying the oscillation frequency is shown to have a large effect on the micromixedness ratio (α) thus maintaining the near micomixing control.

The vertical orientation of the ACR and the high residence times are perceived as issues for plug flow behaviour, however, negligible back mixing and low pressure drops have been validated.

Acknowledgments

Robert Ashe and David Morris of AM Technology are thanked for providing equipment and giving permission to publish the experimental results.

AM Technology
Unit 18, Berkeley Court,
Manor Park, Cheshire, WA7 1TQ, UK
Tel: +44 (0) 1928 237420
www.amt.uk

References

Baldyga, J., Bourne, J. R., Walker, B., "Non-Isothermal Micormixing in Turbulent Liquids: Theory and Experiment", *The Canadian Journal of Chem.l Eng.*, **1998**, *76*, 641-649

Taylor, R. A., Penney, W. R., Vo, H. X., "Scale-up Methods for Fast Competitive Chemical Reaction in Pipeline Mixers", *Ind. Eng. Chem. Res.*, **2005**, *44*, 6095-6102

Paul, E., "Reaction Systems for Bulk Pharmaceutical Production", *Chem. Ind*., **1990**, *21*, 320-325

Paul, E., Atemo-Obeng, V. A., Kresta, S. M., Eds. Handbook of Industrial Mixing; Wiley-Interscience: New York, **2004**

Johnson, B., Prud'homme, R., "Chemical processing and micromixing in confined impinging jets", AIChE *J.*, **2003**, *49*, 2264 – 2282

Baldyga, J., and Pohorecki, R., "Turbulent Micromixing in Chemical Reactors—a Review", *Chem. Eng. J*., **1995**, *58*, 183-195.

Bourne, J. R., Yu, S. Y., "Investigation of Micromixing in Stirred-Tank Reactors Using Parallel Reactions", *Ind. Eng. Chemistry Res.*, **1994**, *33*, 41-55.

Fournier, M.-C., Falk, L., Villermaux, J., "A new parallel competing reaction system for assessing micromixing efficiency: experimental approach" *Chem. Eng. Sci*., **1996**, *51*, 5053-5064.

Tipnis, S. K., Penney, W. R., Fasano, J. B., "An Experimental Investigation to Determine a Scale-Up Method for Fast Competitive Parallel Reactions in Agitated Vessels", *AIChE Symp. Ser.*, **1994**, *299*, 78-91.

Nouri, L'H., Legrand, J., Benmalek, N., Imerzoukene, F., Yeddou, A.-R., Halet, F., "Characterisation and comparison of the micromixing efficiency in torus and batch stirred reactors", *Chem. Eng. J.*, **2008**, *142*, 78-86.

Boss, J., Czastkiewicz, W., "Principles of scale-up for laminar mixing processes of Newtonian fluids in static mixers", *Int. Chem. Eng.*, **1982**, *22*, 362–367.

Song, H.-S., Han, S.-P., "A general correlation for pressure drop in a Kenics static mixer", *Chem. Eng. Sci.*, **2005**, *60*, 5696-5704.

Tatterson, G., "Scaleup and Design of Industrial Mixing Processes", McGraw-Hill, Inc., **1994**

Lin, W. W., Lee, D., J., "Micromixing effects in aerated stirred tank", *Chem. Eng. Sci*., **1997**, *52*, 3837-3842.

Pope, S. B., "Turbulent Flows.", Cambridge University Press, **2000**.

Baldyga, J., Bourne, J. R., "Simplification of Micromixing Calculations. I. Derivation and Application of New Model", *The Chem. Eng. J*., **1989**, *42*, 83-92.